Air pollution and mobility in the Mexico City Metropolitan Area, what drives the COVID-19 death toll?

C. Vladimir Rodríguez-Caballero[a,c,*], J. Eduardo Vera-Valdés[b,c]

[a]*Department of Statistics, ITAM, Mexico*
[b]*Department of Mathematical Sciences, Aalborg University, Denmark*
[c]*CREATES, Denmark*

Abstract

This paper analyzes the relation between air pollution exposure and the number of deaths due to COVID-19 in the Mexico City Metropolitan Area. We test if short- and long-term exposure to air pollution is associated with a higher number of deaths due to the pandemic. Our results show that long-term exposure to particle matter of ten micrometers and smaller are associated with a higher death toll due to the pandemic. Nonetheless, in the short-term, the effect of air pollution on the number of deaths is less pronounced. Once we control for the short-term commonality among municipalities, contemporaneous air pollution exposure is no longer significant. Moreover, we show that the extracted unobservable common factor is highly correlated to mobility. Thus, our results show that mobility seems to be the main driver behind the number of deaths in the short-term. These results are particularly revealing given that the Metropolitan Area did not experience a decrease in air pollution during COVID-19 inspired lockdowns. Thus, this paper highlights the importance of implementing policies to reduce mobility and air pollution to mitigate health risks due to the pandemic. Mobility constraints can reduce the number of deaths due to COVID-19 in the short-term, while pollution policies can reduce health risks in the long-term.

This version: December 6, 2020.

JEL Classification: Q53; Q28; C21; C23.

Keywords: COVID-19; Pollution; Morbidity; Spreading; Mobility.

[*]Corresponding author: Río Hondo No.1, Col. Progreso Tizapán, Álvaro Obregón, CDMX, Mexico. 01080.

Email addresses: vladimir.rodriguez@itam.mx (C. Vladimir Rodríguez-Caballero), eduardo@math.aau.dk (J. Eduardo Vera-Valdés)

1. Introduction

The COVID-19 pandemic is one of the most serious health crisis in recent memory. The official death toll worldwide surpassed 1.5 million as of December 3, 2020, with one death reported every nine seconds on a weekly average. Considering reporting problems in some countries, the actual death toll may not be known for several years. Even though the pandemic is still ongoing, much knowledge has been gained in the past few months. The most prevalent comorbidities seem to be hypertension, diabetes, cardiovascular and respiratory diseases; see Farias Costa et al. (2020); Chudasama et al. (2020); Yang et al. (2020), among others. Furthermore, some evidence has been obtained regarding the effect that air pollution has on morbidity. At the local level, the evidence collected seems to point to a positive correlation between the level of air pollution, particularly Particulate Matters (PM, hereinafter), and the death toll due to COVID-19. To name a few, Yao et al. (2020), Gupta et al. (2020), Bianconi et al. (2020), and Son et al. (2020) find a positive correlation between exposure to PM 2.5, inhalable particles with diameters of 2.5 micrometers and smaller, and a higher number of deaths for the United States, Italy, and Asian Cities. In contrast, Rodriguez-Villamizar et al. (2020) do not find evidence of an association between long-term exposure to PM 2.5 and COVID-19 mortality rate at the municipality level in Colombia, while Vera-Valdés (2020) finds there is no evidence at the macro-level. Moreover, the evidence of the effect of PM 10, inhalable particles with diameters of 10 micrometers and smaller, and SO2, sulfur dioxide, on the number of deaths is less established.

This paper adds to the literature by testing if air pollution levels in the Mexico City Metropolitan Area (MCMA, hereinafter) are associated with a higher number of deaths due to COVID-19. The particular characteristics of the MCMA in terms of its high level of workers in the informal sector, the high number of public transport users, and the high population density make it an interesting edge case. The paper tests the effects of PM 10, PM 2.5, and SO2 on the death toll due to COVID-19 in the MCMA. We assess the effects of long- and short-term exposure to pollutants on the death toll due to the pandemic.

We use a cross-sectional analysis to test if long-term exposure to air pollutants is associated with a higher COVID-19 death toll. Our results show that long-term exposure to all air pollutants is associated with a higher death toll due to COVID-19. The effect seems larger and more significant for PM 2.5, in line with similar studies for other countries. Moreover, once we control for all air pollutants, only PM 2.5 seems to remain significant.

Furthermore, we use panel data models with cross-sectional dependence to analyze the effects of contemporaneous exposure to air pollution on the number of deaths due to the pandemic. Our findings indicate that pollutants are not statistically significant in explaining the death toll in the short-term once we control for the common factor. Moreover, we identify that the unobservable common factor is highly correlated to mobility (proxied by public transport mobility). Consequently, we argue that in the short-term, pollutants are not the main driver behind the number of deaths, but the mobility due to the commercial activities and the lifestyle of the dwellers of the region.

Our results are closely related to the ones from López-Feldman et al. (2021). Using a probabilistic specification, the authors find that long-term air pollution exposure, measured by PM 2.5, increases the probability of death due to COVID-19 in the MCMA, particularly for the elderly. Nonetheless, the authors' results regarding contemporaneous exposure are less clear. In this regard, our results in long-term exposure are in line with the ones from the authors, while we provide a clear explanation behind the lack of short-term effects.

Overall, we provide two warnings to policymakers based on our findings.

⇒ First, long-term exposure to air pollutants is associated with a higher COVID-19 death toll. Thus, we highlight the importance of systematically reducing air pollution exposure to mitigate the risk of death from the current and future pandemics. In short, pollution-reducing policies can lessen health risks in the long-term.

⇒ Second, this pandemic has shown that the worst scenarios are emerging in areas commonly associated with high population density and a highly dynamic lifestyle. Henceforth, to help control the death toll due to COVID-19, we invite governments to implement policies to reduce mobility during the pandemic. Since mobility constraints are the main driver behind the pace of contagion, it can help in reducing the number of deaths due to COVID-19 in the short-term.

2. Materials and Methods

2.1. The Mexico City Metropolitan Area

Mexico City is the capital and largest city of Mexico. The city and its surrounding metropolitan area are the most populous in North America. The exponential population growth began at the beginning of the 20th century due to the strong advantages in terms of social mobility originated by the Mexican Revolution (1920-1920), the physical infrastructure inherited from the time of the Porfirian dictatorship (1876-1910), and the strong economic centralism that is still preserved in the country.

The fastest growth rate in the city occurred in the middle of the century due to industrialization that caused a strong rural to urban migrations. Furthermore, population migrations impacted the growth of some satellite towns in the east and the north of the city. Nowadays, these are still the most crowded zones of the MCMA; see dark red regions in Figure 1. Connolly (2003) reports a clear panorama of Mexico City regarding its origins, economy, and social structure.

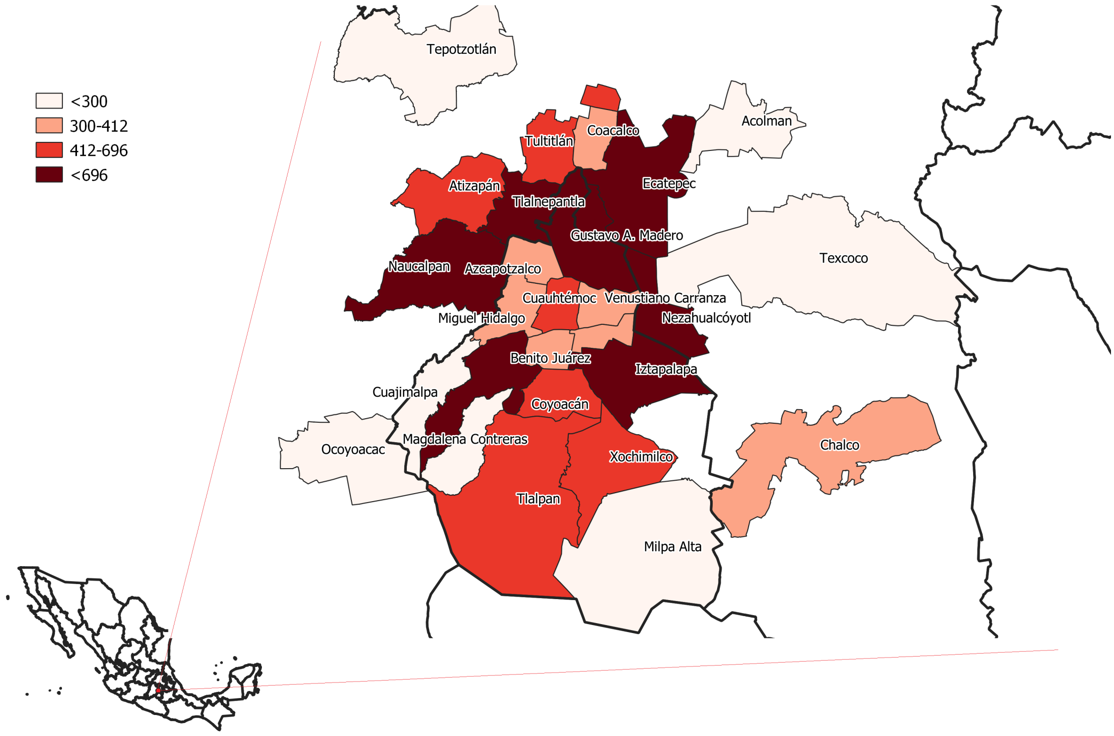

Figure 1: Metropolitan Mexico City's population (in thousands) in 2019. Source: Compiled by the authors using official data from state, municipal, and locality boundary files from the Mexican National Institute of Statistics, Geography and Informatics (INEGI).

The metropolitan-wide transport network is mainly composed of a system of twelve subways lines (Metro, hereinafter), six bus-rapid-transit (BRT) corridors (Metrobus, hereinafter) and another similar BRT system called *Mexibus* that cover some municipalities in the border of the MCMA. The last Metro and Metrobus lines have been planned to connect the areas of higher population density aforementioned with the financial and business districts of the city, which are mostly located in the center: in Benito Juárez, Cuauhtémoc, and Miguel Hidalgo municipalities. Cuajimalpla is another important but satellite city located in the southwestern municipality. However, this part of the city still lacks access to public transport systems like subways, trains, or BRT due to its geographical issues.

Figure 2 reflects the daily dynamics of the city in 2019. Note that Metrobus corridors are represented by green colors and Metro lines in blue. Furthermore, the wider the lines, the more mobility in the system. As seen, there is a decrease in the intensity of the mobility in these public transports on weekends, showing that during non-working days, the financial and business districts are less crowded.

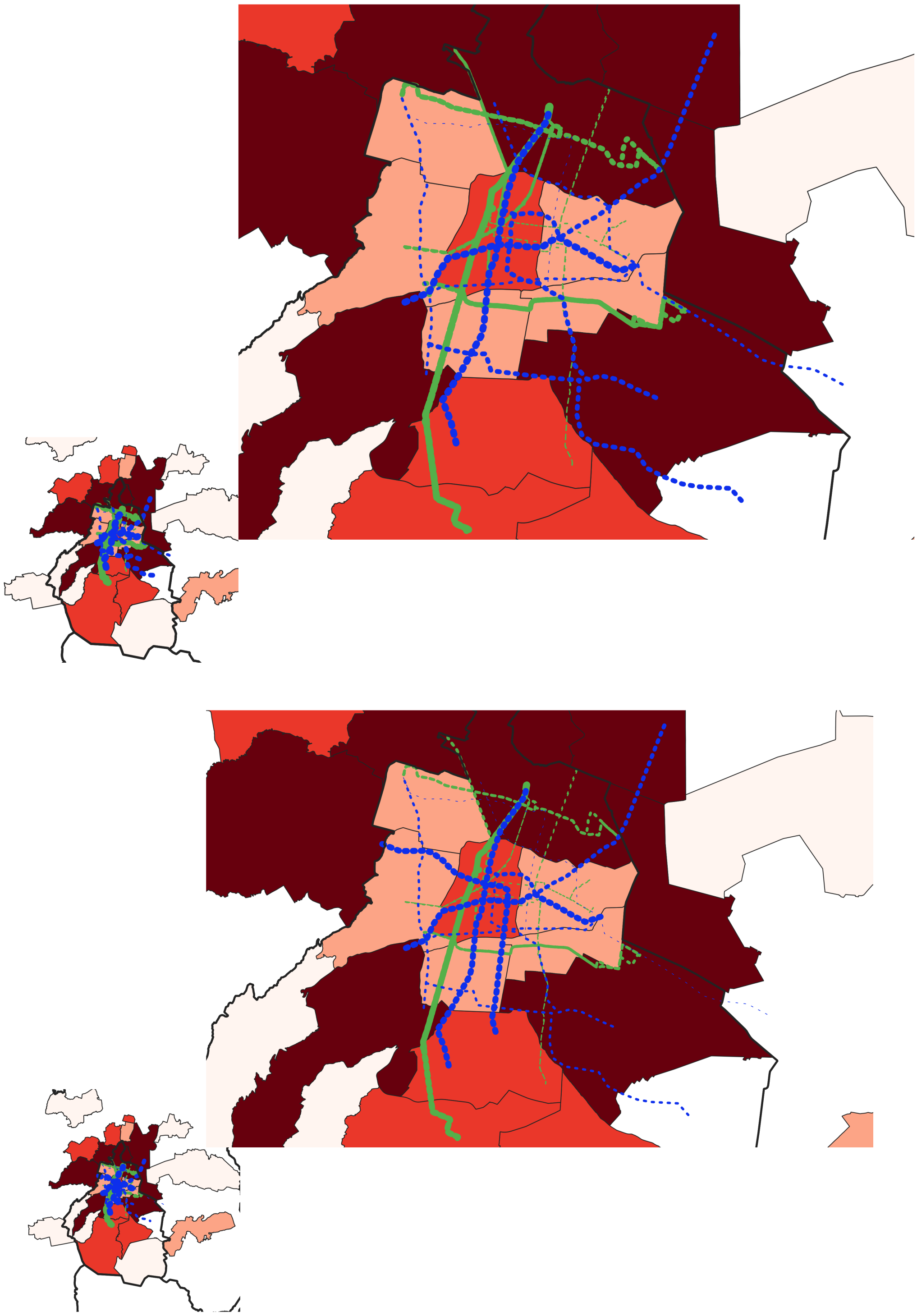

Figure 2: Plots of the annual average of public transport mobility on weekdays (top panel) and weekends (bottom panel) in the Mexico City Metropolitan Area in 2019. Metro and Metrobús lines are indicated in blue and green colors, respectively. The wider the color lines, the more mobility in the Metro or Metrobús.

Air quality is one of the city's biggest problems, even after diverse environmental policies have been implemented in the last four decades. Located in a valley surrounded by mountains and an average altitude of 2200 meters above sea level, the city's irregular topography does not help disperse pollution. Consequently, air pollution is frequently trapped above the city, allowing pollutants to accumulate with limited ventilation of the basin.

As in any other large city around the globe, pollution is generated by a wide range of industrial and other activities. However, the city's local government has concentrated its efforts to reduce contaminants provoked by the daily dense traffic of one of the heaviest congested cities in the world according to the TomTom Traffic Index[1].

The highest concentration of pollutants is frequently observed in the industrial northern section of the city; see the darkest regions in Figure 3. Even if it is a bit impractical to attribute the sources of pollutants, Molina and Molina (2002), Mugica et al. (2002), Moffet et al. (2008b), and Moffet et al. (2008a) point out that the high concentrations of some contaminant particles in the northern MCMA are a consequence of industrial processes and waste incinerators in the northern part of the city. Furthermore, Guerra (2015) finds that municipalities with a higher proportion of households with one or more cars are located in the south and western sections of the city, which shows that there is a low correlation between municipalities with the highest proportion of households with cars and the most polluting regions of the city.

The evidence of the effect that economic restrictions due to the pandemic had on pollution levels across the world is mixed. Significant reductions in Nitrogen Dioxide are encountered in, among others, Brazil, India, and Spain; see Baldasano (2020), Shehzad et al. (2020), and Nakada and Urban (2020). However, Adams (2020) finds that levels of PM 2.5 did not change in response to a region-wide state of emergency in Ontario, Canada. Meanwhile, Berman and Ebisu (2020) found some small declines in PM 2.5 levels in the US, but the results differ significantly between urban and non-urban counties. Moreover, Wang et al. (2020) find that severe air pollution events still occurred in most areas in the North China Plain even after all avoidable activities in China were prohibited on January 23, 2020. Pointedly, the MCMA did not experience a significant reduction in air pollution measurements during and after the COVID-19 lockdown, see Vera-Valdés and Rodríguez-Caballero (2020). In this regard, the short-term effects of air pollution on the death toll are not the result of less air pollution during the pandemic.

[1] The webpage was consulted on November 2020. The link is `tomtom.com/en_gb/traffic-index/ranking/`

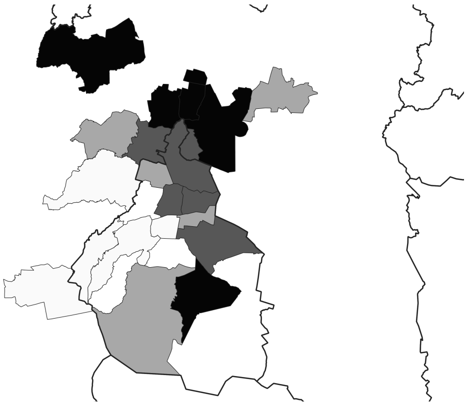

(a)

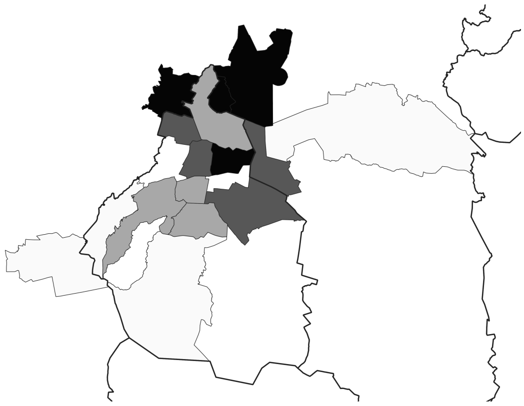

(b)

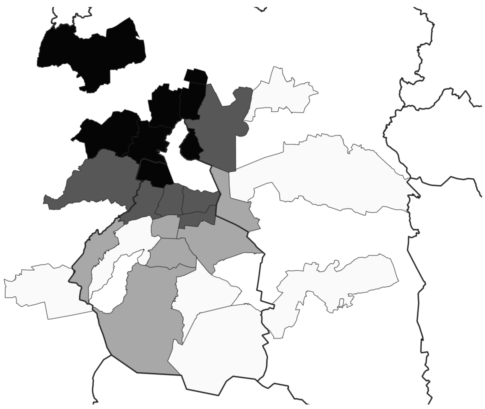

(c)

Figure 3: Plots of annual average of contaminants PM 10 (panel a), PM 2.5 (panel b), and SO2 (panel c) in ppb in the Mexico City Metropolitan Area in 2019. Source: Compiled by authors using data by Mexico City's Automatic Air Quality Monitoring Network (RAMA)

2.2. Mobility Restrictions Due To COVID-19

To slow the spread of contagion, the Mexican Government established "La Jornada Nacional de Sana Distancia" (JNSD, hereinafter) on March 23, 2020; see Secretaría de Salud (2020). The plan established four measures to mitigate the effects of COVID-19 on the general population. The actions considered were:

(i) Personal hygiene recommendations.
(ii) Suspension of activities deemed non-essential.
(iii) Postponement of mass gathering events (more than 5,000 participants).
(iv) Guidelines for care of the elderly.

The goal of the plan was to impose social distancing measures and reduce the spread of the virus. The preventive measures ended on May 30, 2020. JNSD produced a fall in public transport usage of more than half, see Vera-Valdés and Rodríguez-Caballero (2020) and Figure 5. That is, mobility was greatly reduced following the government's recommendations. Nonetheless, as previously argued, the reduction in mobility was not accompanied by a reduction in air pollution levels. Thus, this paper aims to disentangle the effect of short- and long-term air pollution and mobility restrictions on the number of deaths due to COVID-19.

2.3. Data

The data comes from Mexico City's data repository, available online at datos.cdmx.gob.mx. We gathered data on air pollution (PM 10, PM 2.5, and SO2) levels at all stations and the number of deaths due to COVID-19 for every municipality. The data is updated to July 31, 2020. Furthermore, we collected data on the number of passengers at all Metro and Metrobus stations.

The long-term exposure analysis data was constructed considering the mean values for air pollutants in the last 20 years and the total number of deaths, as of July 31, 2020, for each municipality.

For our short-term exposure analysis, we collect the daily air pollution measurements at stations across the MCMA and the number of cases and deaths due to COVID-19 for each municipality. The panel data runs from January 12 to July 31.

3. Results and Discussion

3.1. Health Risks Due to Long-Term Exposure to Air Pollution

This section analyzes if long-term exposure to air pollutants is associated with a higher death toll due to the pandemic using a cross-sectional analysis. As described in Section 2.3, the cross-sectional data considers the average level of exposure to air pollutants in the last 20 years and the total number of deaths due to COVID-19.

We consider the model given by:

$$Deathtoll_i = \alpha + \beta_1 PM10_i + \beta_2 PM2.5_i + \beta_3 SO2_i + \epsilon_i, \quad (1)$$

where i is the index for the municipality. We consider the effect that each pollutant may have on the number of deaths at a municipality level. The hypothesis is that higher exposure to air pollutants in the last years increases the risk of death due to COVID-19.

Results from the long-term exposure analysis are reported in Table 1.

Table 1: Long-term exposure estimates

	Dependent variable:			
	Deathtoll†			
	M1	M2	M3	M4
PM 10	21.32***			12.45
	(5.57)			(7.21)
PM 2.5		72.16***		56.88*
		(16.78)		(28.49)
SO2			33.13	-11.22
			(20.71)	(12.14)
Constant	21.80	-692.14*	706.136***	-798.22
	(218.52)	(374.73)	(138.93)	(443.92)
Observations	16	14	16	14
R^2	0.326	0.558	0.151	0.633

Notes: Robust Newey-West standard errors in parentheses.

*p<0.1; **p<0.05; ***p<0.01.

† Divide by 10^6 to get the death toll per million inhabitants.

For robustness, the table considers four variations of the model presented in Equation (1). We consider a separate specification for each air pollutant and a joint specification. Note that some municipalities do not report PM 2.5 or SO2, so the sample size is smaller for M2 to M4. Furthermore, the table shows the Newey-West robust p-values and standard errors.

The table shows that long-term exposure to all air pollutants is associated with a higher death toll due to COVID-19. The effect seems to be larger and more significant for PM 2.5, in line with similar studies; see Yao et al. (2020); Gupta et al. (2020); Bianconi et al. (2020); López-Feldman et al. (2021), among others. Moreover, once we control for all air pollutants in M4, only PM 2.5 seems to remain significant.

Overall, our results show that long-term exposure to air pollutants is associated with a higher COVID-19 death toll. These results point to the importance of reducing air pollution exposure to reduce the risk of death from the current and future pandemics. Nonetheless, the cross-sectional data is quite limited, as shown in the small degrees of freedom. In this regard, the next subsection increases the degrees of freedom by considering the effect of contemporaneous exposure to air pollutants on the number of deaths in a panel data setting. Moreover, the panel data setting allows us to isolate possible short-term dynamics product of the restrictions imposed to control the spread of COVID-19.

3.2. Health Risks Due to Short-Term Exposure to Air Pollution: Extracting Common Factors

This section considers a panel data approach to evaluate the effect that contemporary exposure to air pollutants has on the death toll due to COVID-19. To assess the aforementioned effects, our interest in this section is twofold: i) controlling for time-invariant factors called fixed effects, such as population density, average income level, etc. ii) allowing for a high degree of commonality among municipalities because it is implausible to assume that the level of air pollutants or death toll between municipalities are independent of each other.

Cross-sectionally correlated errors were originally considered as nuisance parameters when modeling panel data models; see Phillips and Sul (2003) and Moon and Perron (2004). In contrast, the "Panel Analysis of Nonstationarity in Idiosyncratic and Common components" (PANIC) approach proposed by Bai and Ng (2004) considered cross-sectional dependence as an object of interest. It is crucial to consider such dependence to guarantee a consistent estimation independently of the cross-sectional dimension's size, as highlighted by Hsiao and Tahmiscioglu (2008) and Phillips and Sul (2007), among others.

In the last two decades, with the advent of complex macroeconomic and financial datasets, the literature has focused on studying high-dimensional panel data models whose cross-sectional units are not independent of each other. To investigate such models, it is often assumed that unobservable common factors drive the cross-sectional dependence. The applied literature frequently uses two popular approaches to estimate these factors and augment the model with these factor estimates.

A first approach is the Common Correlated Effects Mean Group (CCEMG) method of Pesaran (2006) that uses cross-sectional averages of the observable variables as good proxies for unobservable common factors. The original framework is based on stationary variables, but some extensions allow for non-stationary variables (Kapetanios et al. (2011), Ergemen and Velasco (2017)) and more general factor structures (see Rodríguez-Caballero (2020) and Kapetanios et al. (2020))

A second approach is the interactive fixed effects (IFE) method proposed by Bai (2009). Instead of filtering unobserved common factors by a cross-sectional average of observed variables as in the CCEMG method, the IFE method estimates the common component together with the structural parameters of the panel model using Principal Component Analysis (PCA), which requires a priori knowledge of the number of factors.

In this analysis, we use CCEMG and IFE methods to investigate whether contemporary exposure to air pollutants affect the death toll using the panel data set explained in Section 2.3. Figure 4 shows scatter plots from each air pollutant against each municipality's daily number of deaths. The figure hints at a possible association from PM 10 and PM 2.5 to the number of deaths due to COVID-19. The graphical evidence for the effect of SO2 on the number of deaths is less clear.

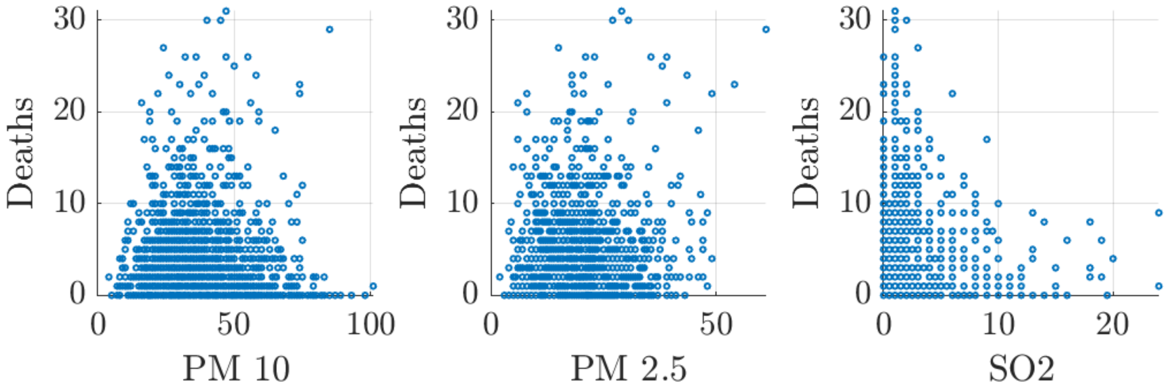

Figure 4: Scatter plots for pollutants and number of deaths due to COVID-19 in the Mexico City Metropolitan Area.

To test if contemporaneous exposure to air pollutants is associated with a higher death toll, we consider the model detailed below.

Let the subindex (i, t) be the observation on the i-th municipality at time t for $i = 1, \ldots, 21$; $t = 1, \ldots, 137$; and consider the following linear panel data model with cross-sectional dependence

$$
\begin{aligned}
Deathtoll_{it} &= \alpha_i + \beta_{1,i} PM10_{i,t-15} + \beta_{2,i} PM25_{i,t-15} + \beta_{3,i} SO2_{i,t-15} + e_{it}, && (2)\\
e_{it} &= \lambda_i^{'} F_t + \epsilon_{it}, && (3)
\end{aligned}
$$

where $Deathtoll$ is the number of deaths due to COVID-19, $PM10$, $PM25$, and $SO2$ are air pollution measurements at stations across the MCMA, with $B = \left(\beta_1^{'}, \beta_2^{'}, \beta_3^{'}\right)$, a vector of unknown coefficients. Furthermore, e_{it} has a factor structure where λ_i is a $(r \times 1)$ vector of factor loadings; $F_t(r \times 1)$ is a vector of common factors so that $\lambda_i' F_t = \lambda_{i1} F_{1t} + \cdots + \lambda_{ir} F_{rt}$; and ε_{it} are idiosyncratic errors. Finally, it is assumed that λ_i, F_t, and ϵ_{it} are all unobserved.

Under Pesaran's approach, the main interest in Equations (2)-(3) is on the inference for the slope heterogeneous coefficients $\beta_{j,i}$ for $j = 1, 2$, and 3 which are computed by

$$\hat{\beta}_i = \left(\mathbf{X}_i'\overline{\mathbf{M}}_w\mathbf{X}_i\right)^{-1}\mathbf{X}_i'\overline{\mathbf{M}}_w\mathbf{y}_i,$$

where $\mathbf{X}_i = (\mathbf{x}_{i1}, \ldots, \mathbf{x}_i T)'$ are the explanatory variables; $\mathbf{y}_i = (y_{i1}, \ldots, y_{iT})'$ the explained variable; and $\overline{\mathbf{M}}_w = I_T - \overline{\mathbf{H}}_w\left(\overline{\mathbf{H}}_w'\overline{\mathbf{H}}_w\right)^{-}\overline{\mathbf{H}}_w'$ the projection matrix, with $\overline{\mathbf{H}}_w = (\mathbf{h}_{w1}, \ldots, \mathbf{h}_{wT})'$ a matrix of cross-sectional averages for the observables. We use simple averages for our estimations; however, weighted averages can be used with more granularity conditions. Then, the CCEMG estimator for a particular pollutant is obtained by $\beta_{CCEMG} = \frac{1}{21}\sum_{i=1}^{21}\beta_i$.

As previously explained, the estimation of latent factors and their loadings are treated as nuisance parameters in the CCE approach. However, it is of particular interest to estimate this latent component in many empirical studies.

A slight difference appears when estimating Equations (2)-(3) by Bai's method. The model assumes that $\alpha_i = \alpha$, $\beta_{1,i} = \beta_1$, $\beta_{2,i} = \beta_2$, and $\beta_{3,i} = \beta_3$. The term *interactive fixed effects* is used to indicate that f_t and λ_i enter the model multiplicatively. As mentioned before, the number of common factors must be specified before estimating the model. In our analysis, we select one common factor.

Besides the slope parameter estimates, we also focus on estimating f_t and λ_i in Bai's method. The estimation is based on a two-step procedure. The first step is to estimate the slope coefficients using the CCE estimator. In the second step, we compute the residuals and use PCA to estimate the factors and loadings. To show that modeling the cross-sectional dependence is a key role in the analysis, we present results from estimating Equation (2)-(3) by Pesaran and Bai's methodologies in Table 2.

The naive model, M0, specifies the standard Mean Groups estimator based on the average of individual time series regressions. These estimates assume that some relevant features such as pollutants in metropolitan municipalities are independent of each other and there are not fixed effects involved in the relationship. Mean group estimates show that the effect of the PM 2.5 contaminant is positive and significant. However, care must be taken since the panel literature has shown that leaving aside the cross-sectional dependence may produce inconsistent estimates.

We continue with the estimation of individual models (M1, M2, and M3) by Pesaran's approach. PM 2.5 and SO2 contaminants are significant in these simple models, but only PM 2.5 is positive; see M2 and M3, respectively. An obvious drawback of these models is that the remaining contaminants are not strictly considered as explanatory variables.

In M4, we estimate the full specification in (2)-(3) by the CCEMG method. We find that only SO2

Table 2: Contemporaneous exposure panel estimates

	Dependent variable: Deathtoll					
	Mean group	Pesaran (2006)				Bai (2009)
	M0	M1	M2	M3	M4	M5
PM10	-0.142***	0.015			0.024	-0.011
	(0.031)	(0.010)			(0.025)	(0.033)
PM25	0.234***		0.050*		-0.042	0.026
	(0.051)		(0.028)		(0.037)	(0.047)
SO2	-0.058			-0.137***	0.183**	0.046
	(0.124)			(0.034)	(0.075)	(0.089)
Constant	4.881***	-0.254	0.030	-0.133	-0.204	0.030
	(1.313)	(0.556)	(0.408)	(0.231)	(0.824)	(1.025)
Observations	1,131	1,738	1,410	2,514	1,131	1,131
R^2	0.547	0.787	0.764	0.757	0.809	0.809

Notes: Robust Newey-West standard errors in parentheses.

*p<0.1; **p<0.05; ***p<0.01.

is positive and significant at 5%, indicating that SO2 has a contemporaneous and positive impact on the death toll. This result complements those findings from López-Feldman et al. (2021) on the MCMA. The authors find that PM 2.5 long-term exposure is a significant factor for death tolls due to COVID-19, whilst the contemporaneous evidence is less firm. Our results suggest that contemporaneously, SO2 may be a more significant health risk factor than PM 2.5.

However, the role that air pollutants have on the death-toll in the short-term may be driven by a common underlying factor not identified in M1 to M4. Thus, we re-estimate the model specified by (2)-(3) while focusing on the estimation of the unobservable factors. Estimates under column M5 correspond to results from Bai's approach. Our findings show that the pollutants are no longer significant once we correctly identify the underlying common factor. To understand why we require a further inspection of the common factor performance.

Figure 5 shows that the unobservable common factor is strongly correlated to the public transport mobility measured as the daily average of all Metro and Metrobus users in the MCMA. The correlation between the common factor and public transport mobility reaches a level slightly above 0.70. Following this reasoning, we argue that, in the short-run, air contaminants are not the main driver behind the death toll but mobility.

Our findings suggest that governments should point to strong and timely restrictions to mobility measures to prevent and contain the spread of COVID-19 in the short-run instead of focusing efforts to control air pollution.

To the best of our knowledge, this paper is the first to analyze the joint effect that reduced mobility and air pollution have on the death toll due to the pandemic. Our results show that governments should introduce mobility restrictions to reduce the number of deaths in the short-term whilst developing policies to reduce air pollution in the long-term. Given the results from this paper and related studies, reducing air pollution levels should be a top priority to reduce health risks associated with respiratory diseases like COVID-19.

Figure 6 displays the weights of the common factor loadings. Note that the signs are all negative. These loadings show that the municipalities with the highest number of deaths have the highest (negative) magnitudes. These loadings indicate the impact of reducing mobility in public transport on the death toll during JNSD. Thus, the policy of mobility restrictions during the JNSD helped to decrease the mortality due to COVID-19. Our findings indicate that these decrements were considerably more relevant in municipalities where people's flux in public transport is high, such as in Iztapalapa and Ecatepec; two regions in the MCMA with the highest rate of population density as detailed in Section 2.1.

Another important observation arises from the factor and loadings estimates. In Mexico, the federal government declared the so-called *third phase* on April 21, 2020, as a consequence of the exponential increase in COVID-19 cases. The contingency plan to fight COVID 19 at this stage consisted of an unforced lockdown, contrary to other countries such as Spain or Italy. In Mexico, the government asked people to stay home and implement social distancing measures. In the third phase, all public events were officially canceled, and more importantly, the government announced the temporary suspension of non-essential activities.

As mentioned in Section 2.1, the daily-life dynamic in the MCMA before the SARS-COV 2 pandemic

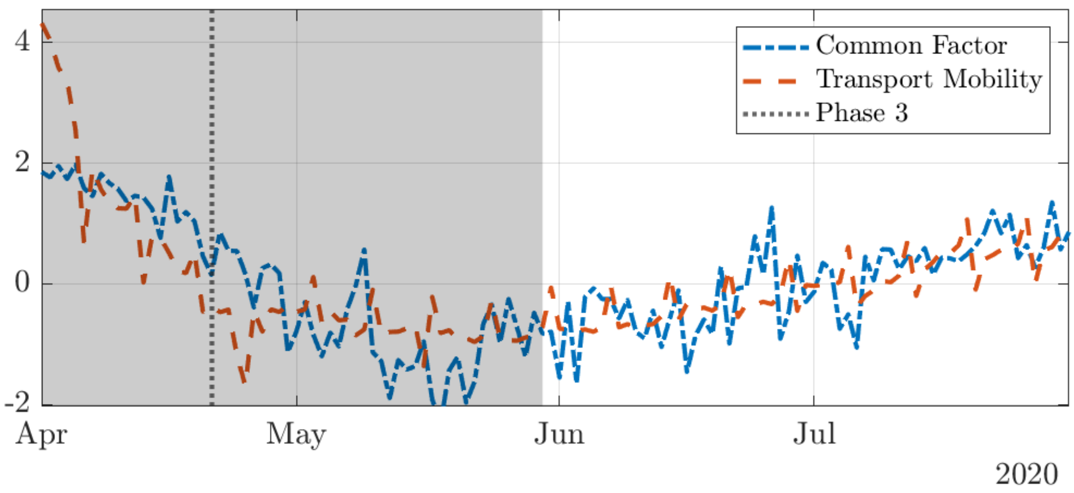

Figure 5: Common factor and transport mobility. JNSD is shown in the shaded area.

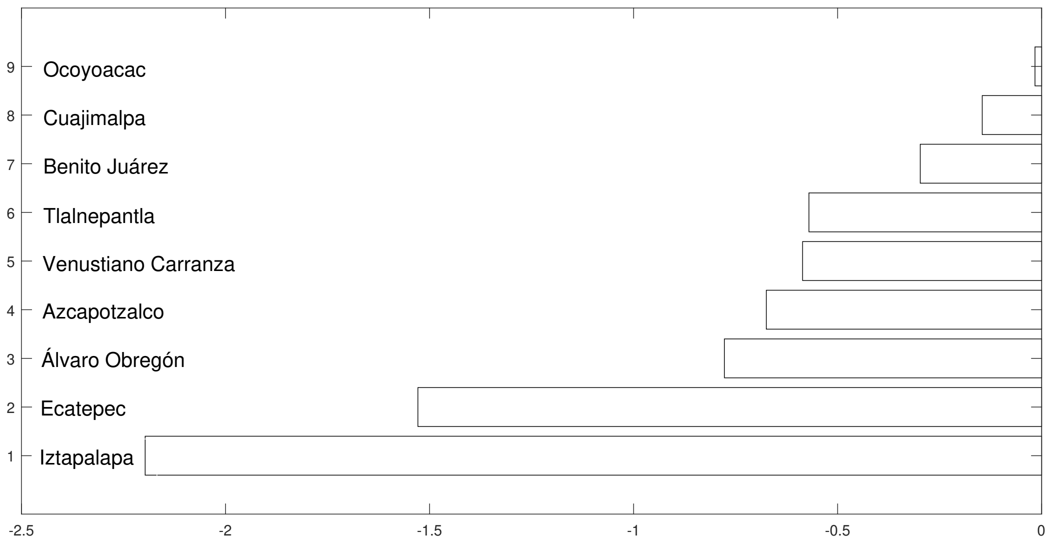

Figure 6: Factor Loadings

showed an important flux of people moving from the periphery of the city (Iztapalapa or Ecatepec) to the business and financial districts (Benito Juarez or Cuajimalpa), particularly on weekdays. However, since the third phase's official announcement, people from the most populated municipalities found conditions to stop moving to the part of the city where most people work as displayed in Figure 6.

When the JNSD officially ended (on May 30), some restrictions announced at the beginning of the third phase were relaxed. Consequently, the flux of people moving from the most crowded part of the city to the financial heart zones increased again. Such an increase in public transport is clearly displayed in Figure 5. The common factor also captures this apparent change in the slope immediately after the shaded area.

Factor loadings may have changed along the period studied due to the constant change in social dynamics, which is not assumed in the panel data model previously considered. To further analyze the loadings' performance, we implement an auxiliary methodology to allow for time-varying factor loadings.

In model M5 of Table 2, we iterate one more time the IFE procedure and estimate a time-varying factor model proposed by Cataño et al. (2019). Their methodology consists of two stages. First, the common factors are estimated by PCA, which is already executed in previous steps in M5. Then, in the second stage, we use these factors to estimate the time-varying loadings by an iterative procedure of generalized least squares and wavelet functions.

The advantage of this approach relies on smooth, progressive variations (smooth deterministic or seasonal trends) that are assumed to drive the behavior of the factor loadings; see Cataño et al. (2019) for more details. Thus, we slightly modify the structure of the specification 3 as follows

$$e_{it} = \lambda_{it}^{'} F_t + \epsilon_{it}, \tag{4}$$

Figure 7 displays time-varying loadings estimates of Equation (4). At first glance, these loadings indicate a smooth variation with a seasonal signal. Cuajimalpa, Benito Juárez, Ocoyoacac share similar behaviors showing local maximums and minimums on similar dates, while the remaining share another dynamic with slightly more seasonal changes along time.

Particularly, in Cuajimalpa and Benito Juárez, we can observe a clear decrease in loadings during the JNSD. Intuitively, the decrease may be related to daily life in both city zones that meet the neuralgic financial and business centers, as explained before. Then, when the third phase started, these municipalities experienced a relevant decrease in people's flux, helping both zones reduce the rhythm of contagion and, consequently, the death toll.

4. Conclusions

This paper analyzes the relation between air pollution exposure and the number of deaths due to COVID-19 in the MCMA. We test if long-term and contemporaneous exposure to air pollution is associated with a higher number of deaths due to the pandemic.

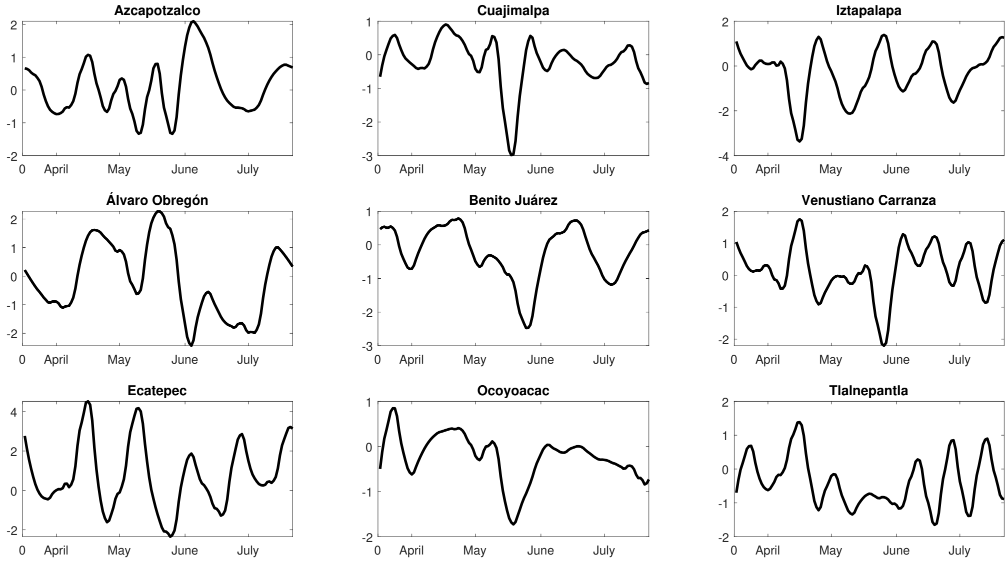

Figure 7: Estimation of the time-varying loadings of model in 4 by Cataño et al. (2019)

Our results show that long-term exposure to air pollutants is associated with a higher COVID-19 death toll. We show that higher levels of air pollution are associated with a higher number of deaths. Nonetheless, our results show that once controlling for PM 2.5, both PM 10 and SO2 are not significantly associated with a higher death toll due to the pandemic. Thus, this paper highlights the importance of systematically reducing air pollution exposure to the smallest particle matters to mitigate the risk of death from the current and future pandemics. In short, pollution-reducing policies can lessen health risks in the long-term.

Moreover, our findings indicate that pollutants seem to be statistically significant to explain the death toll in the short-term when not controlling for a common factor. Nonetheless, once we control for it, our results show that air pollution is no longer significantly associated with the number of deaths. Furthermore, we identify that the unobservable common factor is highly correlated to mobility (proxied by public transport mobility). Consequently, we argue that in the short-term, pollutants are not the main driver behind the number of deaths, but the mobility of the region's inhabitants. These results are particularly revealing given the fact that the MCMA did not experience a decrease in air pollutants during the COVID-19 lockdown.

References

Adams, M.D., 2020. Air pollution in Ontario, Canada during the COVID-19 State of Emergency. Science of The Total Environment 742, 140516. doi:10.1016/j.scitotenv.2020.140516.

Bai, J., 2009. Panel Data Models With Interactive Fixed Effects. Econometrica 77, 1229–1279. doi:10.3982/ecta6135.

Bai, J., Ng, S., 2004. A panic attack on unit roots and cointegration. Econometrica 72, 1127–1177.

Baldasano, J.M., 2020. COVID-19 lockdown effects on air quality by NO2 in the cities of Barcelona and Madrid (Spain). Science of The Total Environment 741, 140353. doi:10.1016/j.scitotenv.2020.140353.

Berman, J.D., Ebisu, K., 2020. Changes in U.S. air pollution during the COVID-19 pandemic. Science of The Total Environment 739, 139864. doi:10.1016/j.scitotenv.2020.139864.

Bianconi, V., Bronzo, P., Banach, M., Sahebkar, A., Mannarino, M., Pirro, M., 2020. Particulate matter pollution and the COVID-19 outbreak: results from Italian regions and provinces. Archives of Medical Science 16, 985–992. doi:10.5114/aoms.2020.95336.

Cataño, D.H., Rodríguez-Caballero, C.V., Peña, D., 2019. Wavelet Estimation for Dynamic Factor Models with Time-Varying Loadings. Technical Report. Department of Economics and Business Economics, Aarhus University.

Chudasama, Y.V., Gillies, C.L., Appiah, K., Zaccardi, F., Razieh, C., Davies, M.J., Yates, T., Khunti, K., 2020. Multimorbidity and SARS-CoV-2 infection in UK Biobank. Diabetes & metabolic syndrome 14, 775–776. doi:10.1016/j.dsx.2020.06.003.

Connolly, P., 2003. The case of mexico city, mexico. Case study report prepared for Understanding Slums: Case Studies for the Global Urban Report .

Ergemen, Y.E., Velasco, C., 2017. Estimation of fractionally integrated panels with fixed effects and cross-section dependence. Journal of Econometrics 196, 248–258.

Farias Costa, F., Reis Rosário, W., Ribeiro Farias, A.C., de Souza, R.G., Duarte Gondim, R.S., 2020. Metabolic syndrome and COVID-19: An update on the associated comorbidities and proposed therapies. Diabetes & Metabolic Syndrome: Clinical Research & Reviews 14, 809–814. doi:10.1016/j.dsx.2020.06.016.

Guerra, E., 2015. The geography of car ownership in mexico city: a joint model of households' residential location and car ownership decisions. Journal of Transport Geography 43, 171–180.

Gupta, A., Bherwani, H., Gautam, S., Anjum, S., Musugu, K., Kumar, N., Anshul, A., Kumar, R., 2020. Air pollution aggravating COVID-19 lethality? Exploration in Asian cities using statistical models. Environment, Development and Sustainability doi:10.1007/s10668-020-00878-9.

Hsiao, C., Tahmiscioglu, A.K., 2008. Estimation of dynamic panel data models with both individual and time-specific effects. Journal of Statistical Planning and Inference 138, 2698–2721.

Kapetanios, G., Pesaran, M.H., Yamagata, T., 2011. Panels with non-stationary multifactor error structures. Journal of Econometrics 160, 326–348.

Kapetanios, G., Serlenga, L., Shin, Y., 2020. Estimation and inference for multi-dimensional heterogeneous panel datasets with hierarchical multi-factor error structure. Journal of Econometrics .

López-Feldman, A., Heres, D., Marquez-Padilla, F., 2021. Air pollution exposure and covid-19: A look at mortality in mexico city using individual-level data. Science of The Total Environment 756, 143929. doi:10.1016/j.scitotenv.2020.143929.

Moffet, R., De Foy, B., Molina, L.a., Molina, M., Prather, K., 2008a. Measurement of ambient aerosols in northern mexico city by single particle mass spectrometry. Atmospheric Chemistry & Physics 8.

Moffet, R.C., Desyaterik, Y., Hopkins, R.J., Tivanski, A.V., Gilles, M.K., Wang, Y., Shutthanandan, V., Molina, L.T., Abraham, R.G., Johnson, K.S., et al., 2008b. Characterization of aerosols containing zn, pb, and cl from an industrial region of mexico city. Environmental Science & Technology 42, 7091–7097.

Molina, L., Molina, M.J., 2002. Air Quality in the Mexico Megacity:: An Integrated Assessment. volume 2. Springer Science & Business Media.

Moon, H.R., Perron, B., 2004. Testing for a unit root in panels with dynamic factors. Journal of econometrics 122, 81–126.

Mugica, V., Maubert, M., Torres, M., Muñoz, J., Rico, E., 2002. Temporal and spatial variations of metal content in tsp and pm10 in mexico city during 1996–1998. Journal of Aerosol Science 33, 91–102.

Nakada, L.Y.K., Urban, R.C., 2020. COVID-19 pandemic: Impacts on the air quality during the partial lockdown in São Paulo state, Brazil. Science of The Total Environment 730, 139087. doi:10.1016/j.scitotenv.2020.139087.

Pesaran, M.H., 2006. Estimation and inference in large heterogeneous panels with a multifactor error structure. Econometrica 74, 967–1012. doi:10.1111/j.1468-0262.2006.00692.x.

Phillips, P.C., Sul, D., 2003. Dynamic panel estimation and homogeneity testing under cross section dependence. The Econometrics Journal 6, 217–259.

Phillips, P.C., Sul, D., 2007. Bias in dynamic panel estimation with fixed effects, incidental trends and cross section dependence. Journal of Econometrics 137, 162–188.

Rodríguez-Caballero, C.V., 2020. Energy consumption and gdp: a panel data analysis with multi-level cross-sectional dependence. Econometrics and Statistics , Forthcoming.

Rodriguez-Villamizar, L.A., Belalcázar-Ceron, L.C., Fernández-Niño, J.A., Marín-Pineda, D.M., Rojas-Sánchez, O.A., Acuña-Merchán, L.A., Ramírez-García, N., Mangones-Matos, S.C., Vargas-González, J.M., Herrera-Torres, J., Agudelo-Castañeda, D.M., Piñeros Jiménez, J.G., Rojas-Roa, N.Y., Herrera-Galindo, V.M., 2020. Air pollution, sociodemographic and health conditions effects on COVID-19 mortality in Colombia: An ecological study. Science of The Total Environment , 144020doi:10.1016/j.scitotenv.2020.144020.

Secretaría de Salud, 2020. Jornada Nacional de Sana Distancia. https://www.gob.mx/cms/uploads/attachment/file/541687/Jornada_Nacional_de_Sana_Distancia.pdf. Accessed: 2020-09-15.

Shehzad, K., Sarfraz, M., Shah, S.G.M., 2020. The impact of COVID-19 as a necessary evil on air pollution in India during the lockdown. Environmental Pollution 266, 115080. doi:10.1016/j.envpol.2020.115080.

Son, J.Y., Fong, K.C., Heo, S., Kim, H., Lim, C.C., Bell, M.L., 2020. Reductions in mortality resulting from reduced air pollution levels due to COVID-19 mitigation measures. Science of The Total Environment 744, 141012. doi:10.1016/j.scitotenv.2020.141012.

Vera-Valdés, J.E., 2020. The Political Risk Factors of COVID-19. International Review of Applied Economics Forthcoming.

Vera-Valdés, J.E., Rodríguez-Caballero, C.V., 2020. Pollution and Mobility in the Mexico City Metropolitan Area in Times of COVID-19. ITAM COVID Working Paper 15, 1–18. URL: centrocovid.itam.mx/es/notas-de-investigacion-centro-covid.

Wang, P., Chen, K., Zhu, S., Wang, P., Zhang, H., 2020. Severe air pollution events not avoided by reduced anthropogenic activities during COVID-19 outbreak. Resources, Conservation and Recycling 158, 104814. doi:10.1016/j.resconrec.2020.104814.

Yang, J., Zheng, Y., Gou, X., Pu, K., Chen, Z., Guo, Q., Ji, R., Wang, H., Wang, Y., Zhou, Y., 2020. Prevalence of comorbidities and its effects in patients infected with SARS-CoV-2: a systematic review and meta-analysis. International Journal of Infectious Diseases 94, 91–95. doi:10.1016/j.ijid.2020.03.017.

Yao, Y., Pan, J., Wang, W., Liu, Z., Kan, H., Qiu, Y., Meng, X., Wang, W., 2020. Association of particulate matter pollution and case fatality rate of COVID-19 in 49 Chinese cities. Science of The Total Environment 741, 140396. doi:10.1016/j.scitotenv.2020.140396.